A New Modality Radar-Acoustic Sensor for Visualisation in Environments with Poor Radar/Lidar Reflectivity

Graham Brooker, *Member, IEEE,* David Johnson, Javier Martinez, Duncan Robertson*, Member IEEE*

***Abstract*— This paper presents a novel 2D imaging sensor for indoor navigation. When complete it will comprise a scanned Radar Acoustic Sounding System (scaRASS) combined with a narrow-beam ultrasound sonar to produce high resolution images using two different modalities. The 40kHz narrow beam scanned sonar generates conventional images based on time-of-flight methods and target reflectivity targets while the RASS produces images based on Bragg enhanced Doppler radar reflections from the acoustic pulse as it travels. The latter technique is suited to imaging low reflectivity objects which scatter or absorb acoustic signals. This combination of modalities ensures that the system is capable of detecting and determining the range and bearing to both high and low reflectivity targets, while the high acoustic frequency, and hence, high attenuation reduce the incidence of long range multipath interference. Additionally the RASS is capable of determining variations in the speed of sound along the path with a commensurate improvement in the accuracy of the acoustic based range measurement. It is also able to measure of the air temperature to a fraction of a degree, allowing it to pinpoint convection currents generated by warm objects**

I. INTRODUCTION

This Reflection of electromagnetic radiation from abrupt changes in atmospheric characteristics is now a well known effect. From the beginnings of radar use during WWII it was one of the phenomena that produced manifestations called "angels" [1]. However, it was not until the late 1950s that the changes in refractive index in air induced by acoustic signals were first identified [2]. Over the next 50 years the phenomenon has been used to produce progressively more sophisticated radio-acoustic sounding systems (RASS) to examine air temperature, wind profiles and turbulence in the lower troposphere [3-5].

By the early 1990s, the technique was being applied to indoor problems [6-8] and the application was being widened to other fields, such as IFF [9] and the detection of wake vortices [10, 11].

It is possible to extend the basic RASS functionality by incorporating an acoustic receiver with an appropriate diplexer to transform the pulsed transmitter into a complete sonar. This is capable of determining the distance to targets within the beam, using conventional time-of-flight principles [12].

This combination of RASS and sonar, in conjunction with a conventional swash-plate scanner [13] produces a novel dual modality 2D imaging sensor that produces images of both low and high reflectivity objects in an indoor environment

Brooker, Johnson and Martinez are with the Australian Centre for Field Robotics at the University of Sydney in Australia (Tel: +612 9351 45023, Fax: +612 9351 7474, gbrooker@acfr.usyd.edu.au). Robertson is with Physics and Astronomy at St Andrews University in Scotland (dar@st-andrews.ac.uk)

II. OPERATIONAL PRINCIPLES - RASS

As an acoustic wave propagates through the air, the density of the medium in one region periodically increases and decreases in a manner which makes these peaks and troughs appear to travel in the direction of propagation.

When an electromagnetic wave passes through the air, in which these acoustically induced changes in density occur, a small fraction of the signal will be reflected at each of the transitions.

A. Bragg Matching

If the wavelengths are matched such that the electromagnetic wavelength is twice that of the acoustic one as illustrated in Figure 1 for $\lambda_e = 2\lambda_a = 16$mm, Bragg matching occurs and reflections sum coherently.

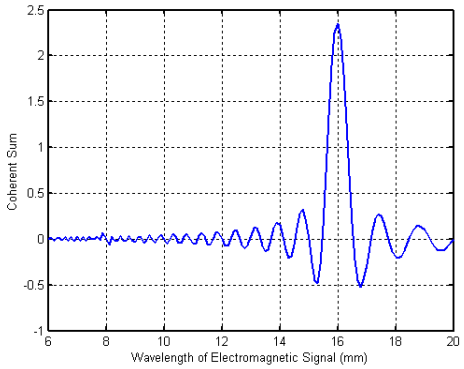

Figure 1. Coherent sum of the reflected signals shows the Bragg Condition

In the RASS case, the Bragg reflector is not static, but a pulse of sound travelling out from the transducer at a velocity $v_a \approx 340$m/s. It is trivial to show that the Doppler shift, f_d (Hz) of the electromagnetic signal is equal to the acoustic frequency f_a (Hz).

$$f_d = \frac{v_a}{\lambda_a} = f_a . \qquad (1)$$

B. Focus Effect

If the acoustic and radar sensors are collocated then the expanding acoustic phase front produces a focusing effect where both the wavefronts expand with the same radius of curvature and so coherence is maintained over the full area of the expanding pulse [9].

According to Clifford [14], the received power, P_r (W) returned from reflection off an acoustic pulse, if the RF beamwidth is smaller than the acoustic beamwidth, can be approximated by

$$P_r = 4.6\times10^{-17}\frac{N^2 P_a P_t}{R^2}\left\{\frac{\sin\left[\left(k_a-2k_e\right)\frac{N\lambda_a}{2}\right]}{\left(k_a-2k_e\right)\frac{N\lambda_a}{2}}\right\}g_a \quad (2)$$

Where P_t is the transmitted RF power (W), P_a the transmitted acoustic power (W), g_a the acoustic antenna gain, N the number of acoustic pulses, R the Range (m), λ_a the acoustic wavelength (m), $k_a = 2\pi/\lambda_a$ and $k_e = 2\pi/\lambda_e$. Marshall [4] provides an identical equation but a factor of three larger.

The radar cross section (RCS), σ_a in m^2, of this expanding acoustic pulse can be determined in terms of the acoustic power, P_a, the acoustic antenna beamwidth, θ_a (rad) and the range, R (m). If the radar beam is wider than the acoustic beam [9] then

$$\sigma_a = 1.69\times10^{-12} R^2\theta_a^2 N^2 P_a \quad (3)$$

C. Atmospheric Attenuation

The equation describing the RCS does not consider the attenuation of the acoustic signal, which increases significantly with increasing frequency [15] [16]. At 40kHz the attenuation varies between 1.1dB/m and 1.4dB/m depending on the relative humidity (RH) and this factor needs to be incorporated into calculations of the effective RCS calculated in (3).

D. Measuring the Range to Low Reflectivity Targets

In environments where the surface reflectivity is too low to generate any significant echo, conventional time-of-flight systems are unable to measure the range to targets. However, as described by [8], the range to low reflectivity targets can be determined by examining the amplitude profile of the received Doppler signature as a function of time (range). In clear air the amplitude decreases at consistent rate dependent on the effective RCS of the acoustic pulse. However on striking an absorbing or scattering medium, the RCS of the pulse decreases abruptly with a commensurate decrease in the amplitude of the Doppler signal. The knee in the RASS amplitude profile defines this range.

D. Measuring Temperature

One of the capabilities of a RASS is to measure the temperature and humidity profiles by measuring the instantaneous Doppler shift as the acoustic pulse propagates through space. The relationship can be rewritten so that the temperature can be determined from the measured speed

$$T = \frac{v_a^2}{402.193}. \quad (4)$$

III. TIME OF FLIGHT SONAR

Time-of-flight sonar relies on the transmission of a narrow beam of acoustic energy and the receipt of echoes from targets (with different acoustic impedance to that of air) within the beam. At its most basic, the range resolution of the sonar is determined by the number of cycles of acoustic energy, generally referred to as the pulse width, transmitted. The range accuracy (to a single point target) is determined by the accuracy to which the speed of sound is known, the signal to noise ratio and the sophistication of the signal processing used to identify the peak of the echo envelope. Some of these techniques are described by Brooker in [17].

The narrow bandwidth of the piezoelectric transmitter and receiver function as pseudo matched filters if the correct number of transmit cycles is used. For a 40 kHz transducer with a bandwidth of 1.5 kHz, a pulse duration of approximately 667 μs is required. This corresponds to about 25 cycles.

IV. SYSTEM CONFIGURATION

The first monostatic configuration tried was to use an annular array of ultrasound transducers surrounding the radar antenna as shown in Figure 2. This configuration produces a very narrow acoustic beam to generate high angular resolution images

Figure 2. Monostatic RASS configuration using a central horn lens antenna surrounded by a double ring of small ultrasound transducers

Unfortunately initial tests showed that attaching the acoustic to the Doppler components of the RASS resulted in significant amounts of coupling between the two, with the result that reverberation within the structure generated large vibrations within the receiver mixer (conventionally described as microphonic effects) that swamped the echoes from the propagating pulse.

Isolation mountings were not effective in reducing microphonics sufficiently, leaving little option but to use the mesh reflector in a space frame structure documented by Weiβ [8].

A. Hardware

The wavelength of an acoustic system operating at 40kHz is 8.5mm so the radar system must operate at a wavelength of 17mm to satisfy the Bragg condition, which equates to a frequency of 17.65GHz. A conventional Doppler radar system with reflected power canceller (RPC) has been constructed

from discrete components, and an array of 131 piezo elements makes up the sonar antenna as can be seen in Figure 3.

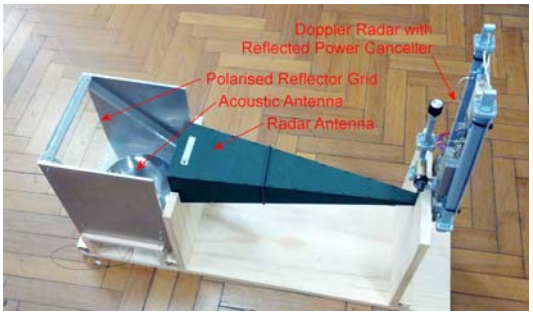

(a)

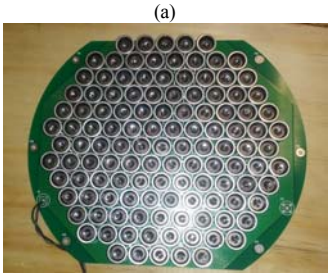

(b)

Figure 3. Photograph (a) of the mesh reflector based RASS and (b) a the 131 element sonar array

The RCS defined in (3) and modified by the atmospheric attenuation produced an RCS is plotted in Figure 4. For an acoustic power of 1 W, it can be seen that the effective RCS reaches a maximum at a range of 6.5m before falling off as the attenuation begins to dominate over the R^2 term. Note however that this RCS is extremely small, reaching a maximum of only -88dBm^2 (1.58×10^{-9} m^2) at its peak in the 25 cycle case.

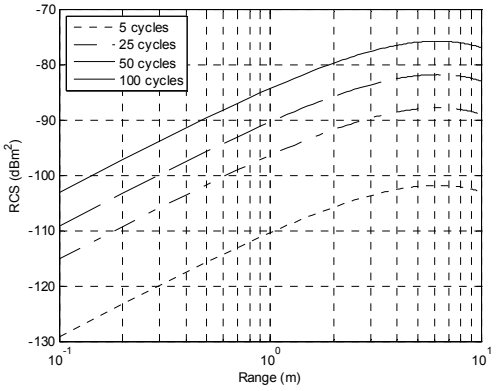

Figure 4. Radar cross section of an acoustic pulse with the number of cycles, N, in a pulse as a parameter

Because the acquisition of the Doppler signal can be synchronized with the generation of an acoustic pulse, it is possible to integrate a large number of measurements to improve the overall signal to noise ratio. For a 10m maximum range, each measurement takes 30ms so it is possible to integrate a number of pulses.

The number of cycles in a pulse should be selected depending on the spatial resolution required and the available SNR as well as the "matched filter" requirement of the sonar

An additional consideration is the range of temperatures expected as these dictate the speed of sound and hence the Doppler shift. For indoor operation a temperature range from 0°C and 45°C should be sufficient. This equates to Doppler shifts ranging from 38.94 kHz to 42.07 kHz that need to be accommodated by the radar.

B. RASS System Calibration

To quantify the system performance, it is convenient to use a Doppler reflector with a known RCS. A conventional moving target would have to move at 340 m/s. In addition, the expected RCS is incredibly small, as can be seen in Figure 4.

To achieve this, a small Doppler target was developed using a 40kHz piezo transducer shown in Figure 5 [18].

Figure 5. Construction of a small Doppler target from a piezo transducer and a small ball bearing

Measurements were made using the Doppler radar, and excitation voltages between 1V and 10V produced variations in the measured RCS ranging from -140.5 dBm^2 and -120.5 dBm^2 as seen in Figure 6.

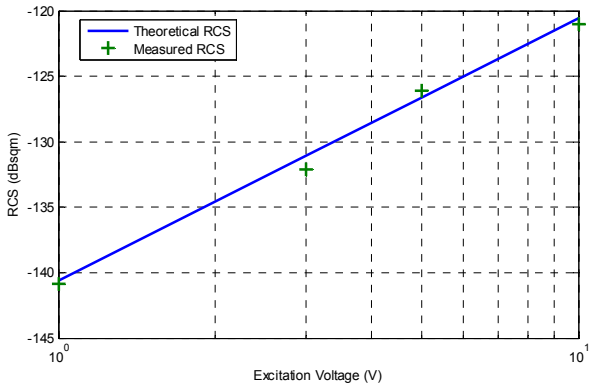

Figure 6. Mean Doppler target RCS at different peak to peak excitation voltages compared to the simulated RCS at the same excitation voltage

V. CONCLUSION

This paper has discussed the ongoing development of a novel indoor dual modality sensor comprising a conventional sonar to detect high reflectivity targets and a RASS to detect low reflectivity targets. It comprises a relatively powerful, narrow beam 40kHz ultrasonic transmitter and an ultra-sensitive Doppler radar combination.

The large acoustic aperture and high frequency result in a narrow beam which allows for the remote measurement of targets within a small volume in space (0.25m×0.25m×0.25m) at a range of up to 10m in the RASS modality. In the sonar modality this is extended to about 30m limited by atmospheric attenuation.

The acoustic sections and the data acquisition system have been completed and good agreement between the measured and modeled characteristics of the acoustic antenna was obtained.

A prototype radar was constructed with the RPC and narrow-band filter, and its performance was measured for a target with known RCS. This measured data was found to be in excellent agreement with the simulated results.

The next phase of the project is to provide a better method of isolating the acoustic transmitter from the Doppler radar to eliminate microphonics and then to provide a method of steering the beam in the azimuth plane to allow dual modality images (sonar and RASS) to be produced.

VI. References

[1] M. Skolnik, *Introduction to Radar Systems*, 2nd ed.: McGraw-Hill Kogakusha, 1980.

[2] A. Tonning, "Scattering of Electromagnetic Waves by an Acoustic Disturbance in the Atmosphere," *Applied Science Res.,* vol. B6, pp. 401-421, 1957.

[3] M. Frankel, N. Chang, and M. Sanders Jr, "A High-Frequency Radio Acoustic Sounder for Remote Measurement of Atmospheric Winds and Temperature," *Bulletin American Meterological Society,* vol. 58, pp. 928-933, September 1977.

[4] J. Marshall, A. Peterson, and A. Barnes Jr, "Combined Radar-Acoustic Sounding System," *Applied Optics,* vol. II, pp. 108-112, January 1972.

[5] N. Bhatnagar and A. Peterson, "Interaction of Electromagnetic and Acoustic Waves in a Stochastic Atmosphere," *IEEE Trans. on Antennas and Propagation,* vol. AP-27, pp. 385-393, May 1979.

[6] M. Daas and R. Knochel, "Microwave-acoustic Measurement System for Remote Temperature Profiling in Closed Environments," in *EUMC*, Helsinki, Finland, 1992, pp. 1225-1230.

[7] M. WeiB and R. Knochel, "A Monostatic Radio-Acoustic Sounding System," *IEEE MTT-S Digest,* vol. THF4-9, pp. 1871-1874, 1999.

[8] M. WeiB and R. Knochel, "A Monostatic Radio-Acoustic Sounding System Used as an Indoor Remote Temperature Profiler," *IEEE Trans. on Instrumentation and Measurement.,* vol. 50, pp. 1043-1047, October 2001 2001.

[9] J. Saffold, F. Williamson, K. Ahuja, L. Stein, and M. Muller, "Radar-acoustic Interaction for IFF Applications," in *IEEE Radar Conference*, Waltham, MA, 1999, pp. 198-202.

[10] R. Marshall, "Wingtip Generated Wake Vortices as Radar Targets," *IEEE AES Systems Magazine,* pp. 27-30, December 1996.

[11] J. Hanson and F. Marcotte, "Aircraft Wake Vortex Generation Using Continuous-Wave Radar," *Johns Hopkins Apl. Technical Digest,* vol. 18, pp. 348-357, 1997.

[12] A. Waite, *Sonar for Practising Engineers*: John Wiley & Sons, 2002.

[13] G. Brooker, M. Bishop, and R. Hennessey, "Evolution of a Suite of Millimetre Wave Radar Systems for Situational Awareness and Automation in Mines," presented at the 2008 Australian Mining technology Conference, Sunshine Coast, QLD, Australia, 2008.

[14] S. Clifford and T. Wang, "The Range Limitation on Radar-Acoustic Sounding Systems (RASS) due to Atmospheric Refractive Turbulence," *IEEE Trans. on Antennas and Propagation,* vol. AP-23, pp. 319-326, May 1977.

[15] L. Kinster and A. Frey, *Fundamentals of Acoustics 2nd Ed*. New York: John Wiley & Sons, 1962.

[16] N. Burnside, "A Function that Returns the Atmospheric Attenuation of Sound," ed: MATLAB Central - http://www.mathworks.com/matlabcentral/fileexchange/loadFile.do?objectId=6000&objectType=FILE, 2004.

[17] G. Brooker, *Introduction to Sensors for Ranging and Imaging*: SciTech, 2008.

[18] G. M. Brooker, "An Adjustable Radar Cross Section Doppler Calibration Target," *Sensors Journal, IEEE,* vol. 15, pp. 476-482, 2015.